Realistic Human Exposure from a 28 GHz and 3.5 GHz Base Station using a Hybrid Ray-Tracer/FDTD method

Robin Wydaeghe[1], Sergei Shikhantsov [1], Emmeric Tanghe[1], Günter Vermeeren[1], Luc Martens[1], Piet Demeester[1] & Wout Joseph[1]

[1]imec - WAVES, Department of Information Technology at Ghent University, Ghent, Belgium

BioEM2022, Nagoya, Japan, June 19-24, 2022

Summary

A hybrid Ray-Tracing/Finite-Difference-Finite-Time (RT/FDTD) method is used to evaluate realistic human exposure to 28 GHz 5G base stations, and compared with 3.5 GHz 5G base stations. Computational costs are drastically increased at 28 GHz. An analysis is made possible by speed optimizations and decreasing the number of simulations. The worst-case scenario (in LOS at 6 m from the base station) is studied. The influence of UE-to-base-station distance, whether the UE is in line-of-sight (LOS) or not (NLOS), and the frequency band is investigated. In the worst-case scenario, the exposure levels did not exceed 9% of its maximum permissible values. The surface absorbed power density at 28 GHz is at most 2.3% of the basic restriction.

Introduction

With the ongoing deployment of 5G, estimating its electromagnetic field exposure is important for public safety. Evaluating *realistic* exposure levels is of interest and compliance with the exposure norms [1] needs to be investigated. Cluster non-stationarity and head coupling need to be accounted for [2], in particular for the NLOS case [3]. The hybrid RT/FDTD method has already proven suitable to capture these effects at 3.5 GHz [2, 3]. 5G base stations also operate at 28 GHz. This work aims to compare and extend these results to the latter *mmWave* frequencies. At these higher frequencies, new challenges need to be addressed: (i) a performance improvement is required, (ii) the absorbed power density (S_{ab} in W/m^2) is used as the relevant exposure metric instead of the peak-spatial specific absorption rate averaged over a 10-g cubic mass ($psSAR_{10g}$ in W/kg).

Methods

Configuration

To facilitate comparison with [3], the same highly reflective environment is used as a model for an indoor factory of the future. Unless otherwise specified, the same parameters, methods, and configurations were employed. Receiving half-wave dipole antennas are similarly positioned along the *x*-axis of the factory. However, the first antenna is placed at a UE-to-base-station separation (henceforth *UE separation*) of 6 m. The blocker in the NLOS case is placed at a separation of 5 m. The reason for this is to study shadowing, especially present close to the blocker. The last receiver is separated by 22 m from the base station. The base station and UEs are placed at a height of 3 and 1.75 m, respectively.

The n77 and n261 frequency bands are used throughout the numerical pipeline. In the following, we refer to these as "at 3.5 GHz" or "at 28 GHz", respectively. Two realistic base stations are modeled that could be installed for 5G coverage at these frequencies. The parameters are shown in Table 1. The antenna configuration is an array consisting of dipole antenna pairs, one for each polarization.

Table 1: Parameters and configuration of the base stations operating in the two frequency bands. The antenna configuration triplet refers to the number of dipoles (1) with a different polarization, (2) along the horizontal direction of the array, and (3) along the vertical direction of the array.

Frequency band	Central frequency (GHz)	Effective bandwidth (MHz)	Total power (W)	Base station model name	Antenna configuration
n77	3.75	900	55 dBm	Ericsson AIR 6449	2x8x8
n261	27.9	800	55 dBm	Ericsson StreetMacro 6701	2x8x12

The parameters used for the RT simulations are shown in Table 2. These parameters are sufficient to accurately predict the channel in the modeled indoor environment.

Table 2: Parameters for the RT simulations.

Frequency [GHz]	Number of reflections	Number of transmissions	Number of diffractions	Threshold [dBm]	Collection radius [m]
3.5	6	2	2	-250	0.20
28	5	2	1	-250	0.20

The same configuration is used for the FDTD simulations as in [3]: the Duke human head phantom with padded cubic free-space bounding box. The head now always faces the negative x-direction, towards the base station. Maximum ratio transmission (MRT) precoding is used to focus the rays 2 cm left of the left ear in a single-user transmission scenario.

Computational costs

The massive MIMO base station requires the knowledge of the wireless channel to perform the precoding. We calculate the channel matrix coefficient as the sum of the signals with different DoAs. A signal is the electric field's z-component received at the location of the UE. The field is computed with a FDTD simulation of a unit plane wave incident on the human head phantom.

Consider the FDTD simulation for one of the DoAs. The wavelength at 28 GHz is about 8 times smaller than at 3.5 GHz. The number of FDTD cells must be at least 8^3=512 times higher to obtain the same number of cells per wavelength. The number of required time steps also increases 8-fold due to the Courant limit. This results in prohibitively large computational costs. Therefore, the execution time of each FDTD simulation at 28 GHz is reduced by a combination of techniques. First, the workflow, including pre- and post-processing, is completely parallelized on a high-performance computing cluster with 40 CPUs and a performant GPU. Second, all results were retained in 196 GB of random-access memory as much as possible, chunking intelligently when exceeding it. Finally, a just-in-time compiler is used along with other code and algorithm optimizations. When possible, the higher frequency is exploited to favorably accelerate the workflow. First, the domain padding is optimized around the phantom to $\lambda/8$, reducing the number of unknowns in the FDTD simulations. The domain padding at 3.5 and 28 GHz is 10 and 1.34 mm, respectively. Second, the ray approximation is more justified at higher frequencies, reducing the number of required rays in the RT simulations. As a result, the number of reflections and diffractions is decreased, as seen in Table 2. Finally, at high frequencies the millimeter-sized voxels overresolve the model's head features. This gives us the freedom to reduce the voxel size to $\lambda/12$, a coarse but acceptable size. The number of voxels at 3.5 and 28 GHz is 2.11 and 30.45 million, respectively.

However, the computing and memory costs remain high. Therefore, the number of FDTD simulations must be reduced. One way to achieve this is by choosing a coarser subdivision of the spherical mesh around the phantom. The 20 faces of the icosahedron of [3] are used as the set of possible discrete DoA angles. In addition, the substantially increased memory load of the electromagnetic field data restricts the number of DoAs, channel realizations and UE separations because, for each of these, the data is exported, added and weighted. Five channel realizations were generated. Nine uniform separations in the *x*-direction between the base station and the UE were considered.

Results

Worst-case scenario

We start by examining a deterministic worst-case scenario in terms of exposure. This occurs when the user is separated 6 m from the base station in a line-of-sight (LOS) case. The channel realization with the worst exposure among the five is chosen. The basic restriction at 3.5 GHz is given by the $psSAR_{10g}$. At 28 GHz, the maximum time-averaged surface absorbed power density S_{ab} (in W/m^2) over a 4-cm^2 surface is used to better account for the superficial nature of the exposure [1]. We present normalized exposure quantities, i.e., for a base station radiating with a total output power of 1 W. Table 3 lists the time-averaged incident power density $|Re(S_{inc})|$ (in W/m^2) in free-space. We define η as the percentual ratio between the simulated exposure quantity and the maximum allowed for the general public (GP), as set by the ICNIRP guidelines [1]. The realistic base stations can emit up to 55 dBm or about 320 W. We find that the values remain below 9% of the maximum exposure guidelines.

Table 3: General public (GP) basic and reference quantities for a deterministic worst-case scenario. The power between rounded brackets indicates the output power of the base station. P_{max} is the base station's total power required to exceed the associated reference level or basic restriction.

	ICNIRP [1] levels for GP	Simulated (1W)	η [%] (1W)	Simulated (320W)	η [%] (320W)	P_{max} [W]
***f* = 28 GHz**						
S_{ab} [W/m^2]	20	1.41e-3	7.05e-3	0.45	2.26	14159
$\|Re(S_{inc})\|$ [W/m^2]	10	2.80e-3	2.80e-2	0.90	8.96	3571
***f* = 3.5 GHz**						
$psSAR_{10g}$ [W/kg]	2	2.43e-4	1.22e-2	7.78e-2	3.89	8226
$\|Re(S_{inc})\|$ [W/m^2]	10	2.08e-3	2.08e-2	0.67	6.65	4812

The maximum power associated to an exposure quantity is found by extrapolating η to 100%. At 3.5 GHz, results are in agreement with [3]. At 28 GHz, the power required to exceed the reference levels in this worst-case scenario is around 14 kW. Today, no commercial 5G indoor base station outputs power at these levels.

Different realistic scenarios

Figure 1 shows the influence of (i) the UE separation, (ii) LOS (blue) exposure compared to NLOS (green) exposure, and (c) the frequency. The time-averaged results from 5 channel realizations are represented by dots. For this number of samples, the mean cannot be deemed statistically significant. However the figures provide some statistical insight, the uncertainty of which is unknown. Graphs (a) and (b) depict a comparison of the reference level quantities at 3.5 GHz on the left and 28 GHz on the right. Similarly, (c) and (d) do so for the basic restriction quantities. The left *y*-axis indicates the relevant exposure quantity. The right *y*-axis represents the percentual ratio η to the maximum permissible value for a realistic base station at 320 W.

The results at 3.5 GHz are similar to those found in [3]. Differences are attributed to the different configurations used. In LOS, the free-space rays dominate. This leads to expected results, e.g., a lower standard deviation. In the NLOS case, shadowing causes the exposure quantities to be highest 12 to 17 m separated from the base station. The distance profiles are highly correlated across frequency and exposure quantity.

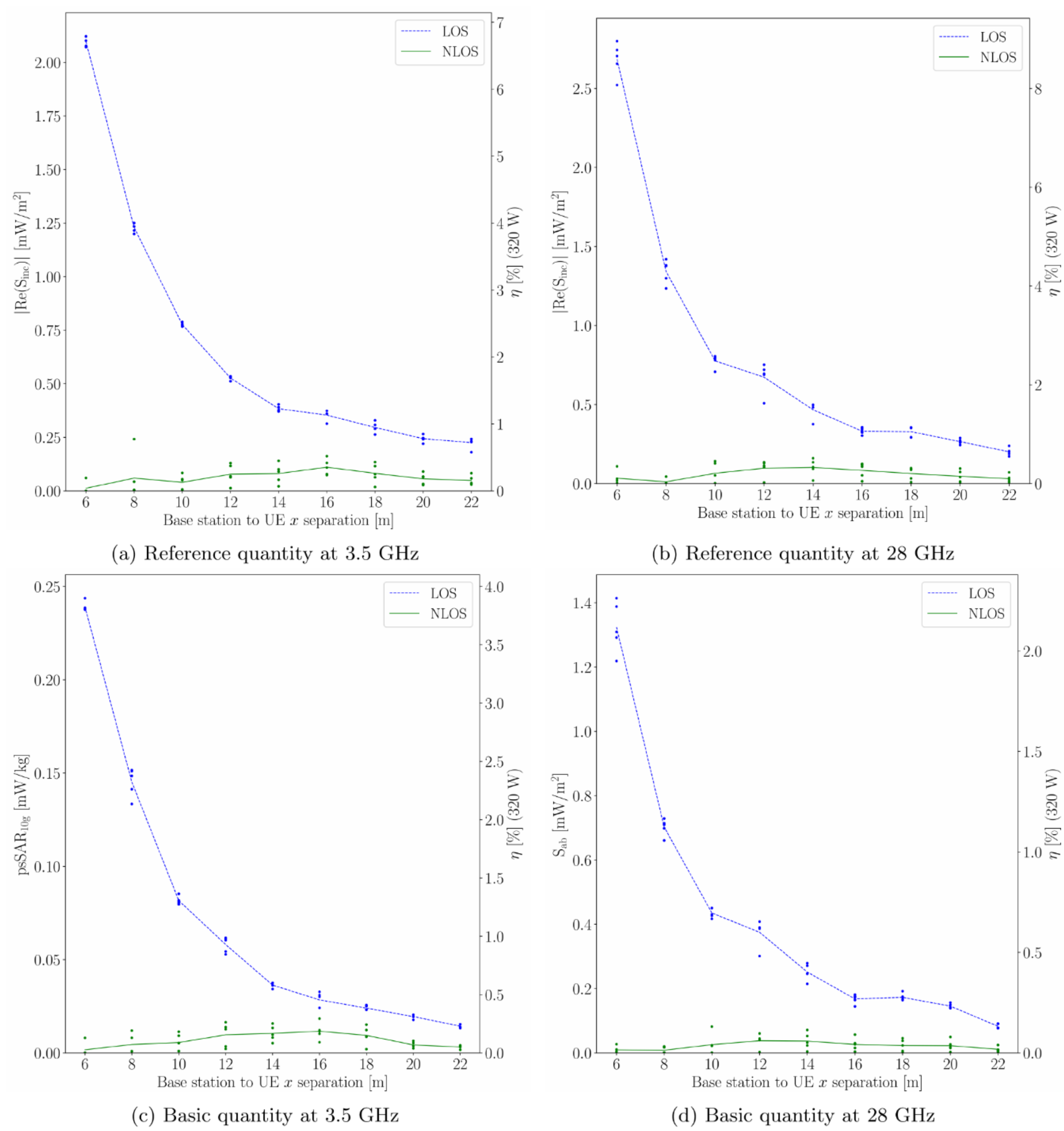

Figure 1: The reference quantities (maximum free-space incident power density, top) and the basic quantities (maximum basic quantities $psSAR_{10g}$ and S_{ab}, bottom) at 3.5 GHz (left) and 28 GHz (right), as a function of horizontally projected UE separation from the base station. Results are normalized for a 1 W base station. The blue and green dots refer to channel realization with LOS or NLOS, respectively. The solid lines connect the means of the LOS or NLOS results of 5 realizations computed for each UE separation. The right y-axis refers to the percentual ratio between the result at 320 W and its maximum permissible value shown in Table 3.

Basic restrictions when the reference levels are met

The ICNIRP guidelines [1] provide reference levels in free-space. When the incident power density is set to this reference level (10 W/m^2), the basic quantities should be below their maximum. Multiplying these with the inverse of η of the reference quantities ($\eta_{\text{reference quantities}}$) is equivalent to setting the reference quantities to the reference levels. This results in the definition of α,

$$\alpha = \frac{\eta_{\text{basic quantities}}}{\eta_{\text{reference quantities}}}.$$

A value of α above 100% means that the basic restrictions would be exceeded if incident power densities are set to the reference levels. This variable is shown as a function of UE separation in Figure 2.

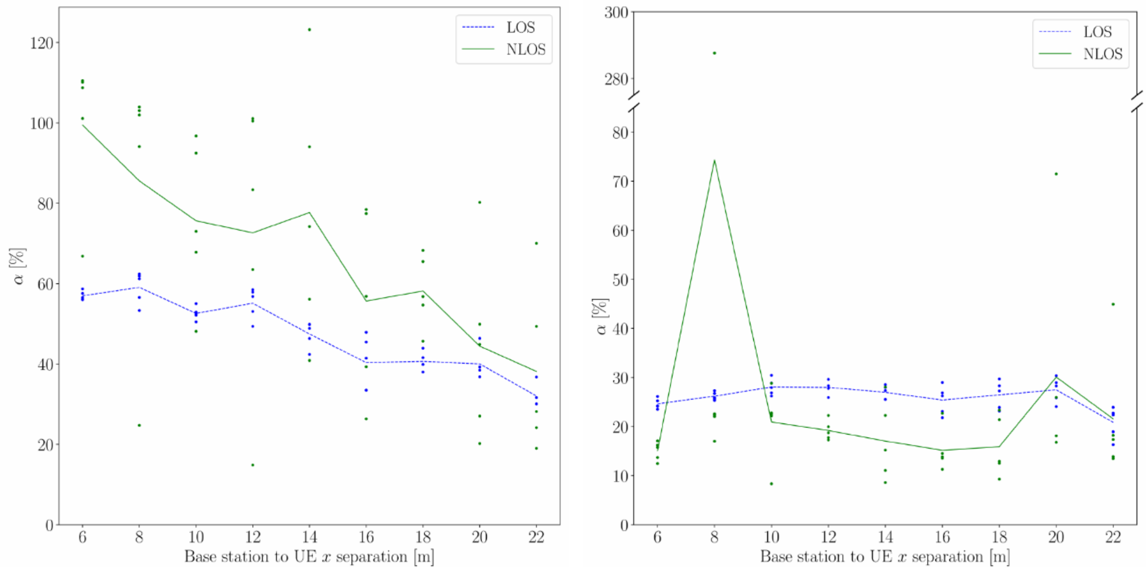

(a) Reference quantity at 3.5 GHz (b) Reference quantity at 28 GHz

Figure 2: The maximum basic quantities when the maximum incident power density equals the reference levels at 3.5 GHz (left) and 28 GHz (right), as a function of horizontally projected UE separation from the base station. The blue and green dots refer to channel realization with LOS or NLOS, respectively. The solid lines connect the means of the LOS or NLOS results of 5 realizations computed for each UE separation.

The results at 3.5 GHz agree with [3]. In the worst-case scenario, α equals 58 and 25% at 3.5 and 28 GHz, respectively. These values coincide with the mean LOS values across distance. The variability of the results across channel realizations is higher in the NLOS case than in LOS.

Conclusions

The high computational costs were sufficiently alleviated to perform a meaningful analysis of realistic human exposure from 3.5 GHz and 28 GHz base stations. The exposure decreases with distance in the LOS case. Shadowing is observed in the NLOS case. In the worst-case scenario, the exposure levels did not exceed 9% of its maximum permissible values. The basic quantity S_{ab} (surface absorbed power density) at 28 GHz is at most 2.3% of the basic restriction. At 28 GHz, basic restrictions are therefore satisfied when the reference levels are met. Future work should aim to increase the number of channel realizations, the resolution in distance and the number of DoA angles. An analysis for multi-user transmission scenarios, different precodings, improving realism through better base station, environment, phantom or UE modeling are options for future research.

Acknowledgements

This work was supported by ERC through "ATTO: A New Concept for Ultrahigh Capacity Wireless Networks" under Grant 695495 and Methusalem through "SHAPE: Next Generation Wireless Networks".

References

[1] ICNIRP, "Guidelines for limiting exposure to electromagnetic fields (100 KHz to 300 GHz)," in Health Physics, vol. 118, no. 5, pp. 483–524, 2020, doi: 10.1097/HP.0000000000001210.

[2] S. Shikhantsov et al., "Massive MIMO Propagation Modeling With User-Induced Coupling Effects Using Ray-Tracing and FDTD," in IEEE Journal on Selected Areas in Communications, vol. 38, no. 9, pp. 1955-1963, Sept. 2020, doi: 10.1109/JSAC.2020.3000874.

[3] S. Shikhantsov et al., "Hybrid Ray-Tracing/FDTD Method for Human Exposure Evaluation of a Massive MIMO Technology in an Industrial Indoor Environment," in IEEE Access, vol. 7, pp. 21020-21031, 2019, doi: 10.1109/ACCESS.2019.2897921.